Investigation of Two Immiscible Liquids Wetting at Elevated Temperature: Interaction Between Liquid FeMn Alloy and Liquid Slag

SARINA BAO, MERETE TANGSTAD, KAI TANG, KRISTIAN ETIENNE EINARSRUD, MARTIN SYVERTSEN, MORTEN ONSØIEN, ARTUR KUDYBA, and SERGEY BUBLIK

The goal of the current work is to develop a methodology to study the wetting behaviour of two immiscible liquids at high temperatures, and to investigate the parameters which influence the wetting properties. The wetting behaviour between synthetic FeMn alloy and synthetic slag has been investigated using the sessile drop technique. Two experimental procedures were implemented under both Ar and CO atmospheres: (a) FeMn alloy and slag placed next to each other on a graphite substrate; and (b) one droplet dropped on top of the other. FactSage is applied to calculate reactions and their equilibrium. The current work presents and demonstrates the suggested methodologies. The results indicate that the wetting between slag and FeMn alloy is relatively stable at temperatures up to 100 K above their melting points, regardless of the droplet size and atmosphere. MnO reduction is accelerated at higher temperature, especially in CO, thus increasing the wetting between FeMn alloy and slag, eventually fusing together. At even higher temperature, slag separates from FeMn alloy due to changing chemical composition during non-equilibrium MnO reduction.

I. INTRODUCTION

IN production of FeMn alloys, which are mostly used for alloying steel, Mn-containing ores are reduced by C materials in furnaces at high temperatures to liquid FeMn alloy. A by-product of this process is a large amount of slag formed by oxides present in the raw materials, typically 600 to 800 kg per tonne of FeMn.[1] During combined tapping of FeMn alloy and slag from the furnace, unwanted entrapment of metal in the slag occurs, as illustrated in Figure 1, which leads to metal losses up to 10 to 15 pct and thus, reduced process yield.

The overall process efficiency is reduced if the separation of slag and metal during tapping is ineffective, since additional energy and operational costs are required to process slag with entrained metal. The entrapment is promoted by unfavourable wetting conditions between liquid slag and metal. By better understanding these liquid-liquid interactions, one can improve the tapping process and thereby the metal yield and process economy. Successful tapping assures high productivity and good profit, *i.e.* stable furnace performance and good melt quality.

The viscosity of FeMn slag is up to 150 dPa s at 1573 K, which readily decreases to up to 50 dPa s at 1673 K.[2] With such sufficiently fluid slag, Jang[3] concluded that metal droplet separation was enhanced by reducing the slag viscosity in FeMn. Similarly, Eidem[4] observed that a slag with an initial lower viscosity, lower MnO content, and higher temperature would have made the settling and the slag-metal separation easier. Thus, measurement of slag viscosity would be of use to study this problem of slag-metal separation during flow. However, surface property (surface tension) than the bulk property (viscosity) will be the focus of the current work in steady state, which in fact related to each other. Ortiz-Young *et al.*[5] had studied water interfacial

SARINA BAO, KAI TANG, MARTIN SYVERTSEN, and MORTEN ONSØIEN are with the SINTEF Industry, Alfred Getz vei 2B, 7034 Trondheim, Norway. Contact email: sarina.bao@sintef.no. SERGEY BUBLIK, MERETE TANGSTAD, and KRISTIAN ETIENNE EINARSRUD are with the Department of Material Science and Engineering, Norwegian University of Science and Technology (NTNU), Alfred Getz vei 2, 7034 Trondheim, Norway. ARTUR KUDYBA is with the Łukasiewicz Research Network - Kraków Institute of Technology, Zakopiańska 73 Str., 30-418 Kraków, Poland.

viscosity on substrates with different wettability. Results demonstrate that boundary viscous forces are related to slippage processes, which in turn can depend on the wettability of the interfacial surface.

It has been shown that the separation of slag and metal during post-tap hole processing could be considerably improved through modification of interfacial properties. For example, Kim et al.[6] found that iron and slag separate from each other due to the decreased wettability between the compounds. Similarly, when the wettability between liquid FeMn slag and alloy decreases, losses during the separation process are estimated to be reduced, and thus the process yield increases. Although many investigations of contact angles and surface tension are available for iron and steelmaking slags and metals,[7–11] these cannot be used for manganese containing systems because of different chemical processes and reactions in HCFeMn slags and alloys.

The driving force in wetting, expressed by contact angle, is the surface tension,[12] the force which minimizes the interface area between different phases.[13] The wettability and adhesion are principally determined by two types of forces,[14] i.e. physical interactions, especially dispersion and polarization forces, and chemical interactions. Physical interactions determine the wettability of low surface tension liquids, for example, water, organic solutions, and hydrocarbons. Chemical wettability is characteristic of high temperature systems and generally shows a strong dependence on temperature.

It is, however, challenging to investigate the wetting of two-liquid systems, in which one liquid displaces another immiscible liquid, as sketched in Figure 2. Even though the individual wetting properties of liquid on solid has been intensively studied for more than 50 years,[15] there is not much research regarding the dynamic wetting between two liquids, beside some studies with oil and water.[16]

In the current work, we develop and demonstrate a methodology for studying the wetting behaviour between immiscible two liquids on laboratory scale, and propose means to alter the wetting properties. This is a continuation of the method developed by Bublik et al.[17] A device designed for examination of high temperature behaviour of liquid metals and their interaction with other ceramics or metals at Centre for Materials Research of Łukasiewicz Research Network - Kraków Institute of Technology (Ł-KIT) in Cracow, Poland* has been applied for this

purpose, in addition to the facilities at SINTEF in Trondheim, Norway.

There are two different ways to measure the wettability following the sessile drop approach. In the contact method (a), two drops are placed next to each, while in the dispensed method (b), a droplet is dropped on top of another. Oxide skins on the samples can be removed[15] in method (a) with fast heating during the first few minutes, while oxide-free liquid[18] from a capillary purification tube can be dropped directly onto the other droplet in method (b), thus minimizing the interaction between two droplets before contact angle measurement. The contact method allows for the interaction between two samples from the solid to the liquid state to be investigated. The spreading kinetics can be studied using the dispensed drop method (b), which allows the process of melting and spreading to be separated so that fully isothermal experiments can be performed. Both techniques will be investigated in the current work.

II. EXPERIMENTAL

Wetting behaviour between liquid metal and slags at high temperatures have been measured by classical Sessile Drop method (Figure 3) combined with two different procedure: (a) Contact method: FeMn alloy and slag pieces are placed next to each other in our wetting lab at SINTEF; (b) Dispensed method: A droplet dropped onto another one on a substrate[19] at the Łukasiewicz Research Network - Kraków Institute of Technology (Ł-KIT)in Cracow, Poland.

Most of the tests have been carried out with method (a) with ISO-88 graphite substrate (or cup in some cases). The classical sessile drop apparatus for method (a), as illustrated schematically in Figure 4, consisted of a two-window stainless steel chamber with graphite heating element and radiation shield, an evacuating system, a gas-in-and-out system, a sample holder, a control C-type thermocouple close to the stage but not touching it, and a pyrometer from one window. The other window was equipped with a digital video camera (Sony XCD-SX910CR, Sony Corporation, Millersville, MD) with a telecentric lens (Navitar 1-50993D) to record images from the molten samples with the resolution of 1280 × 1024 pixels at one frame per second. This means three frames per degree of temperature increase in the current case. The software ImageJ[20] was used to measure the contact angles. The sessile drop furnace was continuously flushed with 0.1 NL/min 6.0 Ar (99.9999 pct purity) or CO (99.9993) gas after evacuated the furnace until 10^{-1} mbar vacuum, and heated up at the heating rate of 300 K/min up to 1173 K and 20 K/min after 1173 K. The samples were cooled in the furnace after the test. Temperature

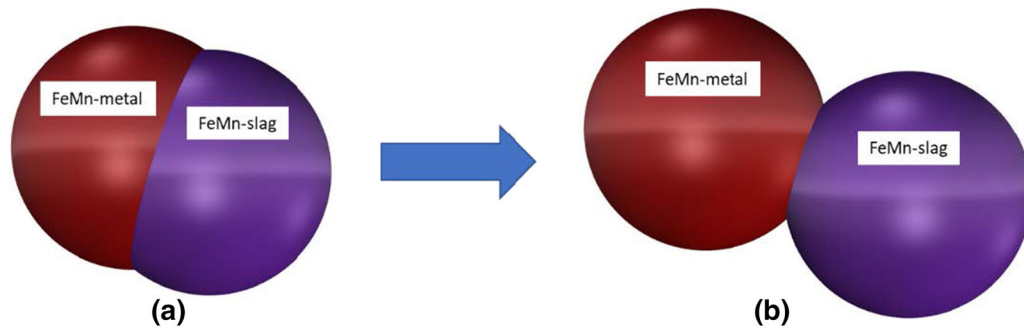Fig. 1—Sketch FeMn droplet entrapment in slag.

Fig. 2—Wetting of two immiscible liquids: (*a*) Good wetting resulting in poor metal yield, and (*b*) poor wetting resulting in good metal yield.

calibration tests with pure Cu and Si have been carried out in both Ar and CO before and after each group of experiments. Subsequently, experimental temperatures were calibrated for all experiments. Note that all the temperatures reported in this work are after calibration. Selected samples have been cut and examined with scanning electron microscope (SEM) with Wavelength Dispersive Spectroscopy (WDS).

Two testes have been carried out with method (b) with ISO-88 graphite substrate, and one with a cup. The sample, together with the graphite substrate, was placed on an alumina sample holder and inserted into the centre of the furnace at room temperate. It was evacuated under a high vacuum of 10^{-6} mbar for two hours to remove any contaminant in the environment. Ar (99.9992 pct, $O_2 < 0.1$ ppm) has been flushed with about 900 mbar pressure in order to avoid evaporation and material loss mainly at temperatures above sample melting point.[19] Four C-type thermocouples located in selected positions surrounding the heater were used to measure the temperature. They were calibrated at the melting point of pure Al, Cu, and Ni. The sample–substrate couple was heated with a rate of 20 K/min. During the experiments, the images were recorded by the high-speed digital CCD camera (Microtron MC 1310, Mikrotron GmbH, Unterschleissheim, Germany) at 50 frames per second. A molten sample was squeezed through a ceramic capillary[18] and dropped on sample at 1623 K. This temperature was kept constant for around 30 min, and then the sample was cooled with a rate of 20 K/s.

FeMn alloy and slag were made from pure chemicals, corresponding to industrial FeMn and slag.[17] Around 100 grams of powders were mixed and melted in a graphite crucible in a graphite tube furnace in argon at 1773 K, which generates C-saturated FeMn alloy and the slag. The same powder mix of FeMn alloy had been melted on a Cu plate in an electronic arc furnace with the same condition, which provides non-C-saturated FeMn alloy. All the product after melting was solidified
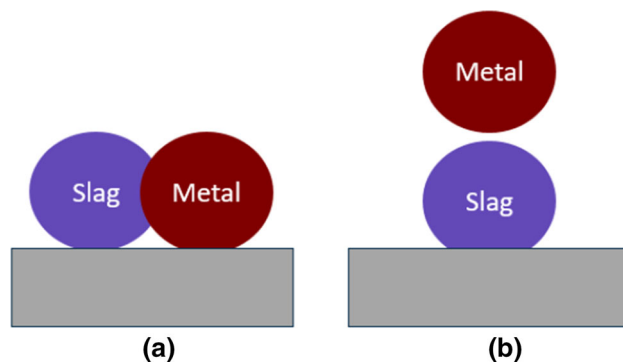

Fig. 3—FeMn alloy and slag placed next to each other on a graphite disc (*a*), and FeMn alloy dispensed onto slag on a graphite disc (*b*).

and crushed. One piece each were taken, embed in epoxy, ground, and analysed by EPMA. Each composition was measured by defocusing an area, and the final values are given as the average of 6 random measurements. Thus, sum of these might be slightly larger or smaller than 100 pct. Even though WDS has high detection limit, carbon analyse has larger uncertainty, because samples were carbon coated, and hydro carbons in the chamber deposit introduce error. Thus, the carbon composition in Table I is indicative as C-saturated (high C) and non-saturated (low C) FeMn in the current case. To get good quantitative values of low carbon, sample with closer composition and the same life cycle should be examined as reference.

Table II presents two FeMn slag compositions with high and low basicity, by doubling the amount of SiO_2 in the initial chemicals. FeMn alloy samples of 28 to 173 mg and slag samples of 13 to 66 mg were used in method (a) on a Ø10 mm ISO-88 standard graphite substrate, while 194 to 255 mg of FeMn alloy and 107 to 129 mg of slag were used in method (b) on a Ø18 mm graphite substrate.
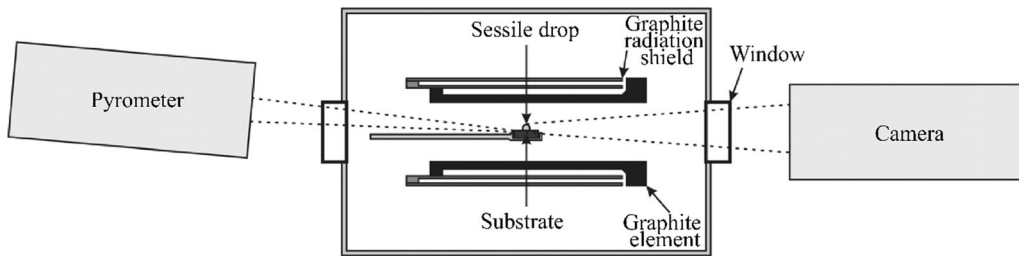
Fig. 4—Schematic of the sessile drop furnace at SINTEF.

Slag and metal phases with above compositions with and without graphite source have been applied in FactSage 8.0[21] to calculate reactions and their equilibrium conditions.

A. Methodology Development

Initially, experiments on both alumina and graphite substrates were performed in order to identify suitable substrates. Slag and FeMn alloy showed clear wetting behaviour on graphite, while the slag droplet reacted with alumina, and then spread around the FeMn alloy. In these cases, it was challenging to observe the wetting between two droplets. Consequently, graphite substrate was chosen for the wetting experiments.

It is worth noting that preparation of synthetic materials should not introduce any additional impurities. Surface-active impurities, such as sulphur or oxygen[22] even in ppm concentration, react intensively at the interface, potentially distorting the measurement of contact angles. Chemical reaction is unavoidable between FeMn alloy and slag according to the thermodynamic calculations. The reactivity is one of the parameters influencing the wettability. Molybdenum foil was placed on the graphite to prevent the dissolution of C from the substrate in FeMn. However, FeMn dissolved the Mo completely. Consequently, our results might have been influenced by C dissolution, as discussed in later sections.

B. Experimental Approach

In this study, three different approaches have been tested for the dispensed method: b1. slag dropping onto the alloy droplet; b2. alloy dropping onto the slag droplet; and b3. slag dropping onto the metal bath in a graphite cup. During holding at 1623 K for 30 min, the contact angle increases and decreases again after the second droplet (Figure 5) for slag dropping and slag dropping onto the metal bath. As expected, lower contact angle between metal and graphite is observed with capillary purification that successfully eliminates the oxide layer of the FeMn alloy. However, solid particles condensation on the metal droplet surface is seen during the isothermal holding. FeMn alloy and slag droplets wet so good that metal droplet still hanging from capillary purification tube drags away the slag droplet during attachment from its original position. This validates our definition of two immiscible liquids, as illustrated in Figure 7.

Table I. Chemical Composition of FeMn Metal Measured by EPMA

FeMn Alloy (Wt Pct)	C	Mn	Fe
Low C	3.3	61.6	34.1
High C	6.7	80.4	14.9

Two approaches have been tested for contact method: a1. two droplets placed next to each other; and a2. slag placed on top of the FeMn alloy layer in the graphite cup. Since slag does not wet graphite as good as FeMn metal, no horizontal slag bath can be made in graphite cup. Instead, a slag ball would form. As can be observed from Figure 6, in dispensed method, slag dropping provides contact angle of 45 to 63 deg compared to metal dropping of 30 to 42 deg. Apparently, capillary purification guarantees the oxide-free FeMn metal droplet, which contributes to lower contact angles in metal dropping. This value overlays with contact angle of two contacted droplets 21 to 45 deg. Thus, both methods are applicable to investigate the wettability between two molten materials. Apparently, slag on metal bath gives larger apparent contact angle, especially after capillary purification, 44 to 74 deg in the contact method and 70 to 104 deg in the dispensed method, respectively. Probably the MnO reduction of slag was not so active since alloy layer separates the slag and graphite contact. Previously, it has been shown that the approach with slag droplet on top of metal bath can be applied to investigate the interfacial tension between slag and metal.[23] This is considered by Bublik in References 22, 24. Thus, both methods are valuable to investigate the wetting of the two immiscible liquids. Most of the works have been carried out with contact method in our wetting lab, SINTEF.

III. PARAMETERS INFLUENCING WETTING

Traditionally, contact angle between a liquid material and a solid substrate is measured as inner angle θ_{sg} as shown in Figure 7, where θ less than 90 deg is defined as a good wetting, and vice versa. Graphite does not wet high C FeMn metal ($\theta_{mg} = 108$ deg) and low SiO_2 slag ($\theta_{sg} = 146$ deg) at their melting points of 1541 and 1543 K, respectively. In this work, the two-liquid contact angle is defined by two tangent lines at their contact point, θ_{sm}, as indicated in Figure 7.

Table II. Chemical Composition of FeMn Slag Measured by EPMA

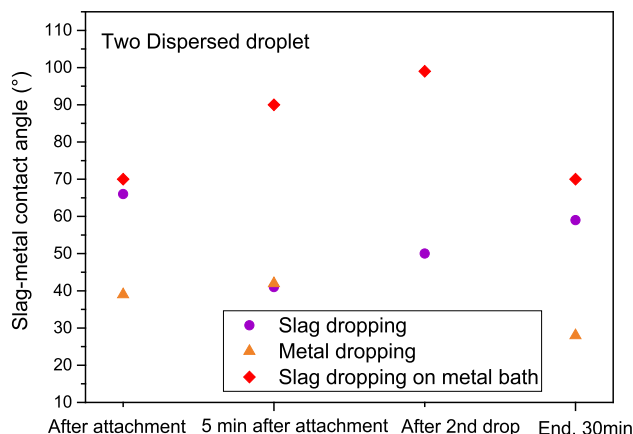| Slag (Wt Pct)	SiO_2	MgO	CaO	MnO	Al_2O_3	FeO
Low SiO_2 Slag	23.0	5.6	22.7	35.2	10.5	0.1
High SiO_2 Slag	39.3	4.0	14.5	35.1	8.0	0.1

Fig. 5—Contact angle of low SiO_2 slag with high C FeMn alloy on graphite in the dispensed method. There was no second drop for metal dropping.
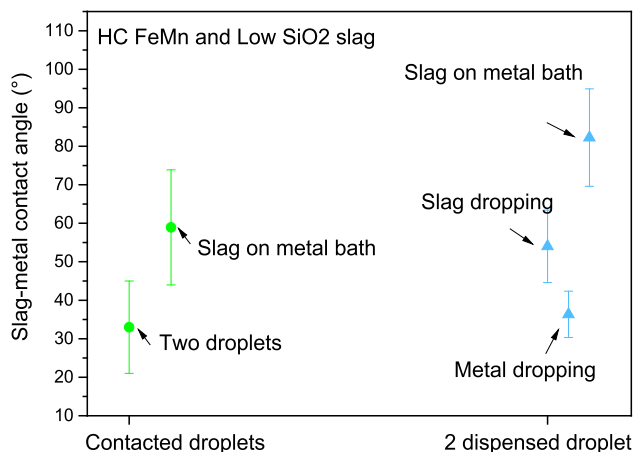

Fig. 6—Contact angle of low SiO_2 slag with high C FeMn alloy on graphite in the dispensed method and the contact method.

A. Temperature

Figure 8 shows that the contact angle is 42 ± 4, 148 ± 6, and 108 ± 2 deg at slag and metal (S/M) weight ratio of 1.10 for slag-metal, slag-graphite, and metal-graphite, respectively, when increasing the temperature from their melting points to approximately 100 K above. This indicates that temperature in this range does not
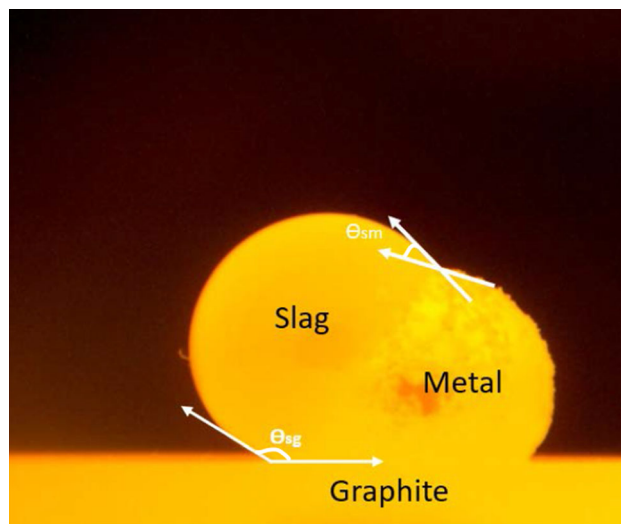

Fig. 7—Wetting behaviour of two immiscible liquids on substrate, where θ_{sg} represents contact angle between slag and the graphite substrate, and θ_{sm} represents contact angle between slag and metal.

influence the wetting of this two-liquid system. The given temperature corresponds to the tapping temperature in industrial FeMn alloy production. The wettability at higher temperatures will change with non-equilibrium reduction, which is discussed in Section III–E.

B. Droplet Size

The wettability of two droplets with slag and metal weight ratio from 0.14 to 1.39 has been investigated with method (a). Each value with its standard deviation in Figure 9 represents one experiment as shown in Figure 8. The slag-metal contact angle spreads in the range of 10 to 80 deg. This indicates that FeMn alloy and slag wets well, and the wetting behaviour does not alter due to the droplet size. Note that FeMn alloy is denser than slag in liquid state. Thus, the weight ratio of slag and metal is different from their volume ratio, as indicated in Figure 10.

C. Atmosphere

The wetting behaviour of low SiO_2 slag and high C FeMn alloy in Ar and CO has been studied with method (a). As shown in Figures 11(a) and 12, relatively stable contact angles for graphite–slag (139 ± 3 deg), graphite–metal, (90 ± 2 deg) and slag–metal (38 ± 5 deg) were observed during the heating above their liquidus, when the slag and metal weight ratio was 0.79 in Ar. However, the reaction is noticeable in CO atmosphere, resulting in a rapid decrease of contact angle between slag and metal from 36 deg, and finally fusing, while θ_{sg} was still 136 ± 6 deg. The reaction in both gases is confirmed with images from a light
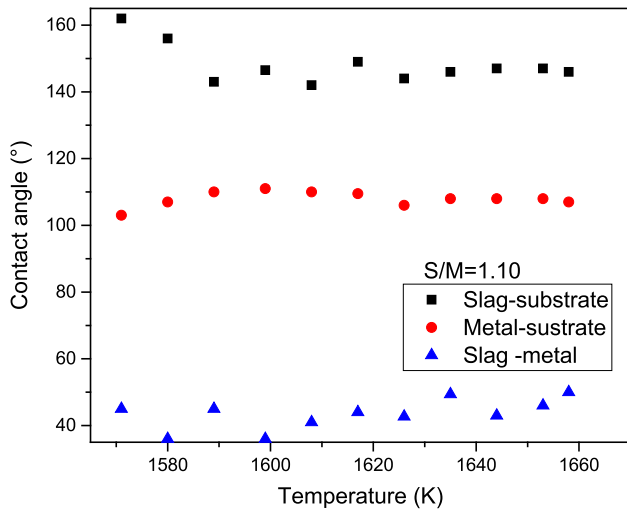
Fig. 8—Contact angle of low SiO_2 slag and high C FeMn alloy on graphite in Ar.
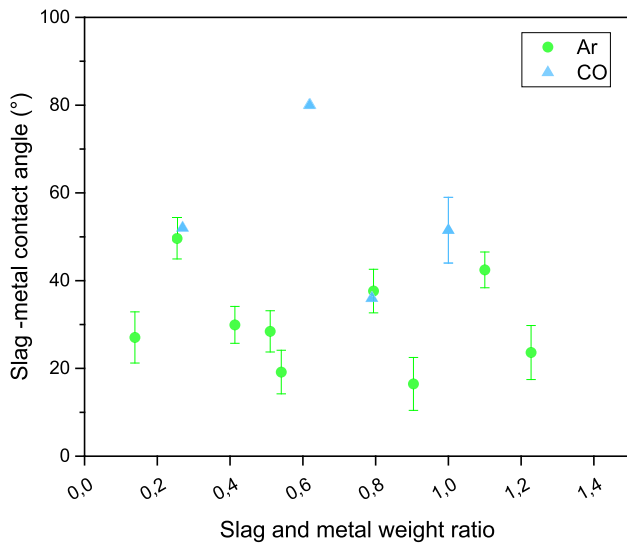

Fig. 9—Contact angle of low SiO_2 slag and high C FeMn alloy on graphite with various slag and metal weight ratio in Ar and CO with method (a) before 1660 K.
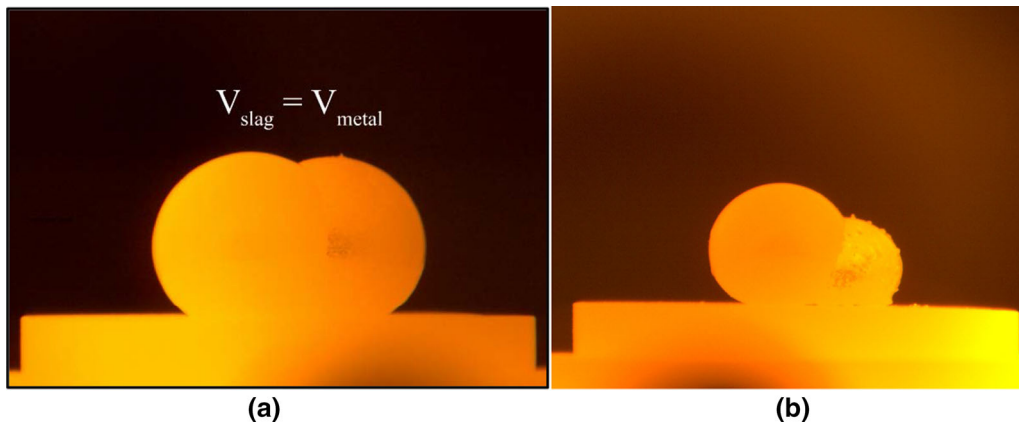
microscopy after the solidification, cf. Figure 11(b) and FactSage calculations, and both samples had the same dendrite in the slag after cooling. Solid particles precipitated on the FeMn alloy surface was observed in both atmospheres, but not on slag. The particles have been confirmed to be solid C.[22]

Again in Figure 9, at temperatures lower than 1660 K where no reduction of MnO has occurred yet, few slag-metal contact angles have been measured in CO. They are mostly within the deviation values in Ar. However, above 1660 K, the active reaction in CO improved the wettability between slag and metal, and contact angle increases with temperature (Figure 13). This will be further discussed in Section III–E.

D. Composition

The contact angle of high (39.3 wt pct) SiO_2 slag with low (3.3 wt pct) C FeMn, can only be measured at temperatures above 1650 K (Figure 13) in both Ar and CO when proper round shape has been shown after their melting. If we look closely at the dynamic wetting in Figure 14, the low C FeMn totally wets high SiO_2 slag after melting, while pushes away the slag when MnO in the slag is reduced both in Ar and in CO atmospheres. This indicates that C saturation or change in composition decreases the wettability (increases the contact angle) between slag and FeMn alloy. In addition, C precipitation has been observed on top of FeMn layer in all experiments. 'Hair' grows heavily on low C FeMn alloy (Figure 14(a)) especially in CO (Figure 14(e)) during melting until slag totally covers it (Figures 14(b) and (f)). The FeMn alloy droplet gradually detaches from slag (Figures 14(c), (d), and (g)) when approaching equilibrium between FeMn and C, while a shell can be observed at the surface of FeMn.

Figure 15 summarizes the contact angle between high (6.7 wt pct) C FeMn alloy and slag containing low (23.0 wt pct) and high (39.3 wt pct) amount of SiO_2. The contact angle varies from 10 to 54 deg in Ar and from 36 to 80 deg in CO atmosphere for both slags at temperature under 1635 K, where no MnO reduction occurs yet. Thus, our results indicate that no significant change of wettability occurs when the SiO_2 amount is doubled,
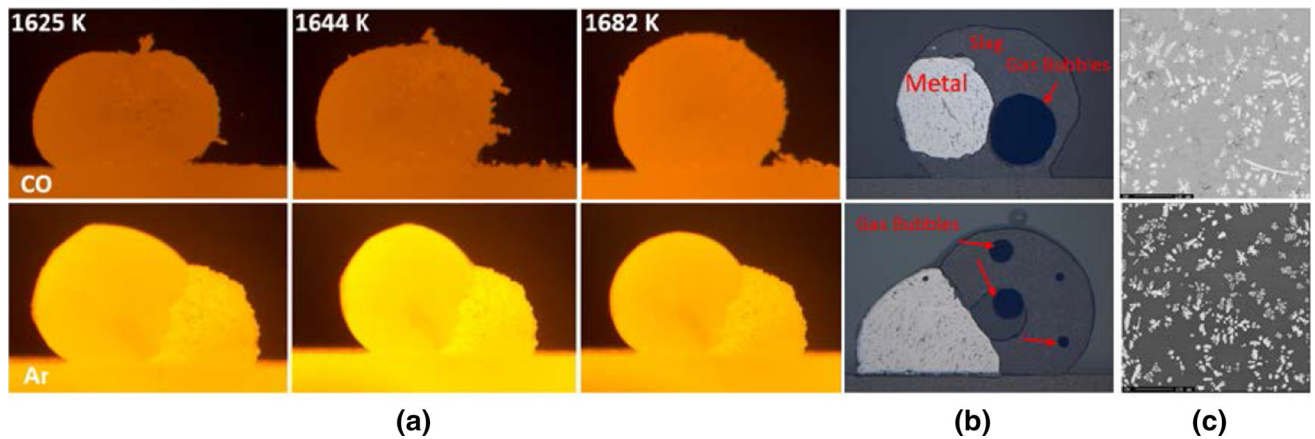

Fig. 10—Slag and metal volume ratio 1 (S/M weight ratio = 0.5 to 0.6) on the left (a) and slag and metal weight ratio 1.1 on the right (b).

Fig. 11—Wetting behaviour between low SiO_2 slag and high C FeMn alloy on graphite in CO and Ar with S/M weight ratio 0.79: (*a*) dynamic wetting with temperature; (*b*) sectioned solid droplets in epoxy, and (*c*) slag consisting of dendrites and homogeneous matrix.
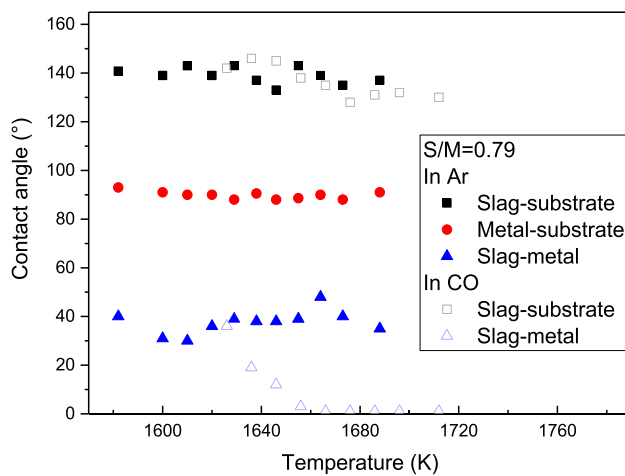

Fig. 12—Contact angles of low SiO_2 slag and high C FeMn alloy on graphite in Ar and CO with S/M = 0.79. Slag had lifted up the metal droplet in CO, thus no valid metal-substrate angle has been measured.
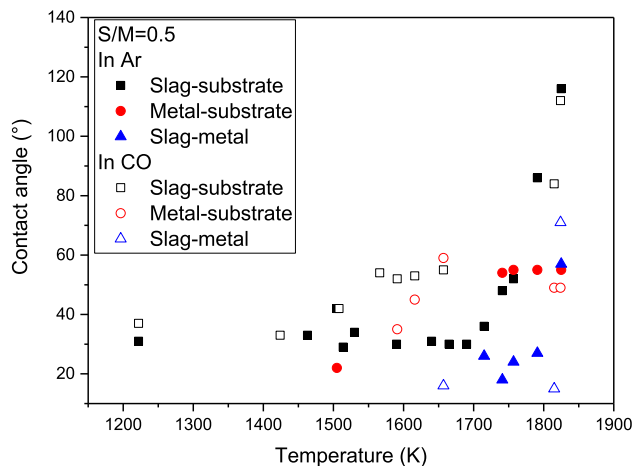

Fig. 13—Contact angles of high SiO_2 slag and low C FeMn alloy on graphite in Ar and CO with S/M = 0.50.

at temperatures up to 1635 K. Additional experiments should be carried out for high SiO_2 slag to further support this observation.

E. Reactions

Equilibrium calculations have been performed in FactSage 8.0 considering 100 g FeMn alloy, 50 g slag and in most cases 20 g graphite, shown in Figures 16, 17, 18, 19, 20 and 21. The commercial databases of FactSage software package, FactPS, FToxid and FSstel, have been used in the equilibrium calculations. For non-ideal mixture phases, only the liquid metal and molten slag have been considered in the present work. The solution phases of SlagA in FToxid and Liquid in FSstel are thus employed in all the case studies. The gas mixture is treated as an ideal mixture in this work.

MnO reduction increases with temperature in all cases with graphite consumption, when it is available. Without solid graphite (Figure 16), MnO reduction started from approximately 1650 K (measured to approximately 1590 K with graphite substrate as seen from Figure 8) in Ar, and ended with 23 wt pct MnO at 1850 K (4 wt pct with graphite substrate) with low silicate slag in Figure 20. Thus, MnO in slag is reduced by C either dissolved in the alloy, or from the graphite substrate, as shown in Reaction [1]. Graphite activates this reduction at lower temperature. However, it is not clear if the solid C directly participates in reduction or after dissolved into FeMn alloy by Reaction [2]. The C saturation rate is relatively fast in FeMn. For instance, Kaffash et al.[25] observed 3 and 5 wt pct dissolved C from graphite within 2 min at 1823 K for Fe-60 wt pct Mn and Fe-85 wt pct Mn, respectively. Generally liquid–liquid reaction rates are much faster than liquid-solid ones, due to the faster interfacial reaction and larger mass transfer in liquid. In our experiments, slag has a larger contact area with alloy (Figure 11(b)), since it does not wet graphite as good as the FeMn alloy. Thus, most likely, the reduction of MnO in slag by dissolved C in metal phase dominates with continuous C dissolution from the substrate. This is supported by Figure 11(b) where gas bubbles are trapped inside the slag, but not all escaped
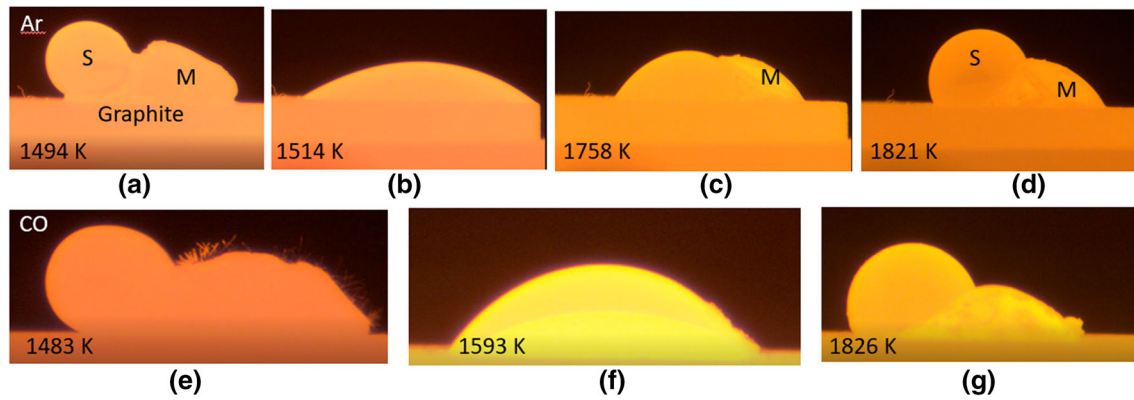
Fig. 14—Interaction between high SiO$_2$ slag and low C FeMn alloy on graphite with S/M = 0.50 during heating in Ar and CO atmospheres. C precipitates (*a* and *e*), two droplets fuse (*b* and *f*), and detaches again (*c*, *d*, and *g*).
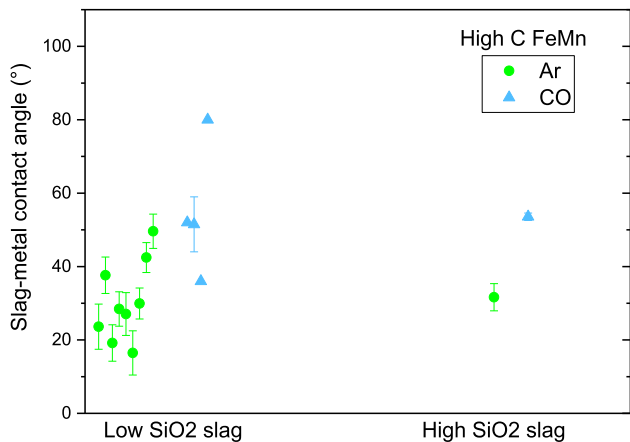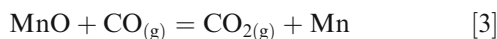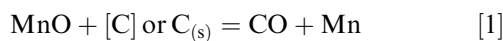

Fig. 15—Contact angle between slag and high C FeMn alloy on graphite before 1635 K.

from the graphite-slag interface after furnace cooling. In Figure 14, the C dissolution and MnO reduction happen at the same time with increasing temperature with low initial C content in FeMn alloy.

$$MnO + [C] \text{ or } C_{(s)} = CO + Mn \qquad [1]$$

$$C_{(s)} = [C] \qquad [2]$$

$$MnO + CO_{(g)} = CO_{2(g)} + Mn \qquad [3]$$

The reduction generally starts at higher temperature in CO, but with higher reaction rates. This is not expected in Reaction [1]. Instead, Reaction [3] dominates with pure CO gas sweeping away the CO$_2$ gas (Figure 21). The calculations were made based on the assumption of unity activities of MnO and partial pressure of CO is equal to 1, except the indications in the figure. As shown in Figure 11(a), slag and metal fuse

together with increasing amount of Mn from reduction Reaction [3], and separate again when composition is changed at higher temperature.

MnO reduction in low silicate slag with high and low C FeMn alloy shows the same path with graphite substrate (Figure 20). This indicates that graphite supplies sufficient amounts of C independent of the initial content of C in the alloy. Mn in the alloy is initially slightly oxidized at 1550 K with high silicate slag, but it is already reduced at 1550 K with low silicate slag. Both slags achieve the same equilibrium MnO amount at 1850 K with greater MnO reduction rate in high silicate slag by temperature.

According to Table III, small amounts of FeO already have been reduced at 1550 K from initial composition (Table II). No SiO$_2$ reduction has been found in these equilibrium calculations. C saturation is 7 wt pct with 14 wt pct Fe-79 wt pct Mn with low silicate slag, and 6 wt pct C saturation with 33 wt pct Fe-60 wt pct Mn with high silicate slag at 1630 K even though it is initiated from 3.3 wt pct C—34 wt pct Fe-62 wt pct Mn in alloy.

Pure CO gas is stable (partial pressure = 1) at T > 1635 K with high silicate slag in Figure 18 left, and T > 1595 K with low silicate slag in Figures 16, 17, and 19 left. This means that the MnO reduction under CO atmosphere can only be stable above this temperate at equilibrium. However, with continuous flushing of CO, MnO reduction seems initiated slightly before that according to Figures 11 and 14.

Even though the MnO reduction by CO in the FeMn process is limited, due to the thermodynamics limitation, it can take place under special conditions. But this has not been broadly studied in the literature. With FactSage ver 5.4 calculation, Safarian et al.[26] observed that ΔG of Reaction [3] is negative for a wide range of MnO activity at high temperatures, as also seen in Figure 21. With the same apparatus and similar condition, they also concluded that when slag is in contact with C in CO, both Reactions [1] and [3] occurs, which
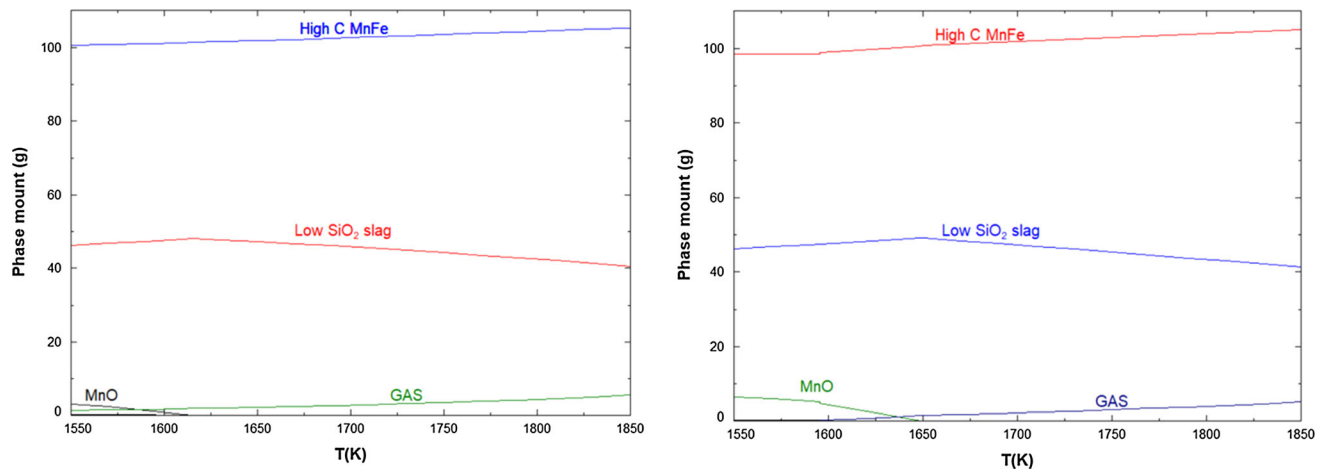
Fig. 16—Phase calculation of low silicate slag with high C FeMn alloy without graphite in Ar (left) and in CO (right) by FactSage 8.0.
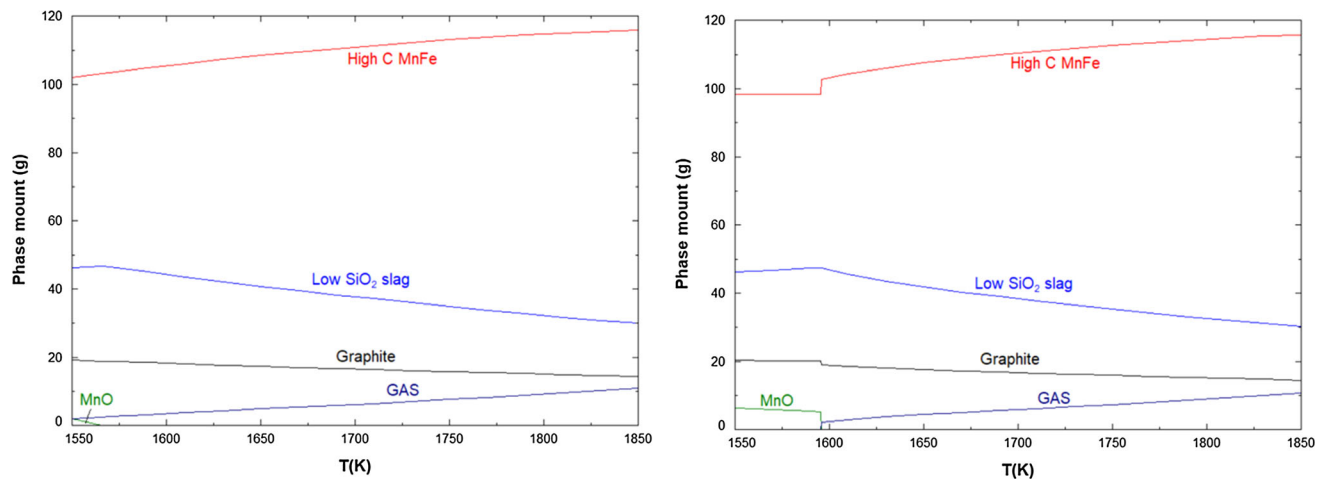

Fig. 17—Phase calculation of low silicate slag with high C FeMn alloy on graphite substrate in Ar (left) and in CO (right) by FactSage 8.0.

give higher reduction of MnO in CO than Ar initially. When activity of MnO is reduced to a certain level, the MnO reduction by CO reduced, and the MnO is mostly reduced by C. Thus, slower reduction of MnO can be observed both in CO and Ar at a low MnO content.

The wetting between slag and metal, slag and graphite, and metal and graphite is expected to be changing, while the slag and metal reaction is occurring. As the reactions stops, the wettability will again be stabilized. To evaluate the wettability one should consider three conditions: before reaction, during non-equilibrium reaction, and equilibrium. If we look closely the case of high SiO$_2$ slag and low C FeMn alloy on graphite in Figures 13, 14, and Table III:

In Ar:

1. At temperatures lower than 1550 K, where the slag and metal compositions are still close to initial compositions, the slag-graphite wetting (contact angle 31 to 42 deg) is relatively stable, when the metal is not fully melted yet (Figure 13).
2. With MnO reduction together with C dissolution from graphite until approximately 1700 K, slag en-

gulfs the metal droplet right after melting, where metal–graphite contact angle is 22 deg, and contact angle of 29 to 34 deg is measured for slag and graphite.
3. With accelerated MnO reduction after 1700 K, slag and metal starts to separate from each other (Figure 14) with contact angle increased from 18 to 57 deg, while both slag and metal are changing their composition (Figure 20). Metal shows stable wetting towards graphite with 55 deg, but slag wetting towards graphite is reduced with contact angles from 36 to 166 deg at 1825 K, when the MnO has been reduced to 5.7 wt pct. FactSage calculations give MnO amount of 4.3 wt pct at 1850 K.

In CO:

1. When the MnO content in slag is still close to initial compositions at temperature below 1550K, the slag-graphite wetting (33 to 42 deg) is relatively stable.
2. Slag covers the FeMn alloy during its melting up to 1591 K with accelerated reduction by CO according to Reaction [3], and its contact angle with graphite
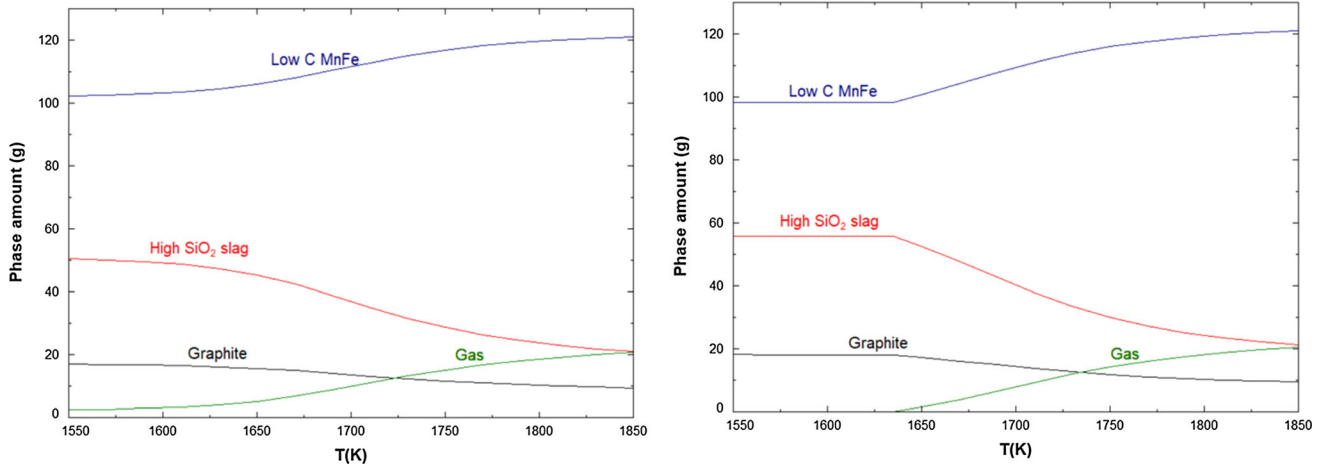
Fig. 18—Phase calculation of high silicate slag with low C FeMn alloy on graphite substrate in Ar (left) and in CO (right) by FactSage 8.0.
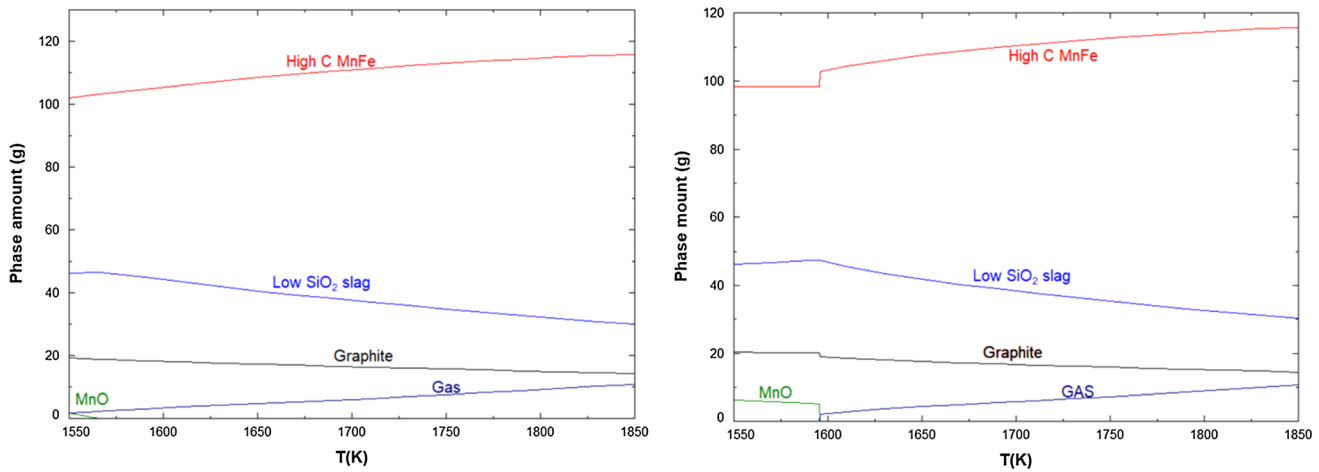

Fig. 19—Phase calculation of low silicate slag with low C FeMn alloy on graphite substrate in Ar (left) and in CO (right) by FactSage 8.0.
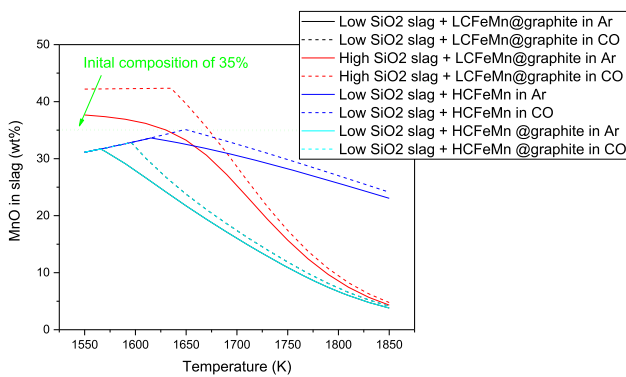

Fig. 20—MnO amount in slag with temperature by FactSage calculation. Lines for low SiO_2 slag and LCFeMn (in black) and low SiO_2 slag and HCFeMn (in light blue) duplicate with each other. This indicates the C supply from the graphite (Color figure online).
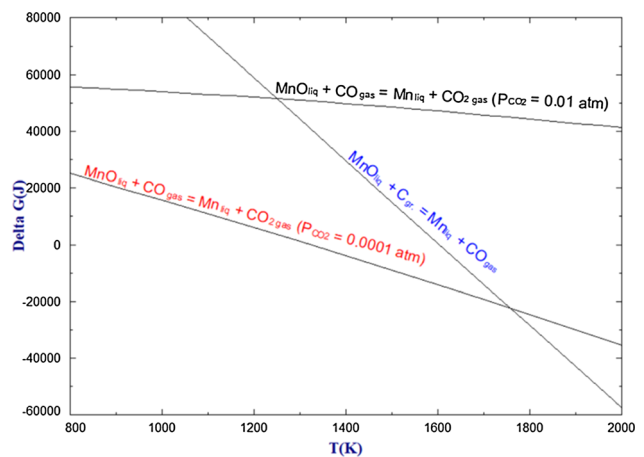

Fig. 21—Gibbs free energies of Reactions [1] and [3] calculated by FactSage.

Table III. Phase Amount With Temperature Initiated With low C FeMn Alloy

	In Metal (Wt Pct)			In Slag (Wt Pct)					
	C	Fe	Mn	Al_2O_3	SiO_2	CaO	FeO	MgO	MnO
High Silicate Slag, 1550K	6.1	33.7	59.7	7.9	36.3	14.2	0.004	3.9	37.7
Low Silicate Slag, 1550K	6.9	14.3	78.7	11.7	25.6	25.3	0.002	6.2	31.1
High Silicate Slag, 1630K	6.1	33.0	60.1	8.4	37.3	15.2	0.006	4.2	35.0
Low Silicate Slag, 1630K	7.1	13.6	79.3	12.9	28.2	27.9	0.002	6.9	24.2
High Silicate Slag, 1850K	5.1	28.5	61.6	18.8	33.3	34.3	0.001	9.2	4.3
Low Silicate Slag, 1850K	7.0	12.6	79.1	18.0	29.7	39.0	0.0007	9.5	3.8

becomes 52 to 54 deg. The contact angle of metal and graphite increases from 35 to 59 deg after melting.

3. Slag and metal droplets start to separate after 1635 K with contact angles increasing from 16 to 71 deg with further accelerated MnO reduction by CO gas, while the contact angle of metal-graphite stabilizes at 49 deg. Slag gets increasingly non-wetting until 112 deg at 1825 K, when the MnO has been reduced to 6.3 wt pct by equilibrium calculation. It further gives MnO amount of 4.8 wt pct at 1850 K. Then the reduction slows down again according to Reaction [1], similar to that in Ar.

Under non-equilibrium conditions, the free energy changes for the system are associated with decrease in the corresponding interfacial tension. However, after the completion of reaction at the interface followed by its continuation into the bulk regions by diffusion, the specific interfacial energy and interfacial tension gradually increase towards their static values.[27] Thus, contact angles at the interface are expected to change in non-equilibrium conditions, and then stabilize when equilibrium is achieved.

compositions of slag and metal. Small amounts of FeO have been reduced at early stages. No SiO_2 reduction has been found in these equilibrium calculations.

The dynamic wetting of two immiscible liquids is going through three different reaction steps: before reaction, during non-equilibrium reaction, and finally equilibrium. However, we can not conclude that equilibrium is achieved in the current experiments.

1. At temperatures where the slag and metal compositions are still close to initial compositions, silicate slag wets FeMn alloy. The wettability is stable (θ_{sg} and θ_{mg}) during the first 100 K above melting points of FeMn and slag.
2. With increasing temperature, and hence slag reduction, slag covers the metal droplet due to MnO reduction.
3. With further increasing temperature, slag and metal separate from each other at presumably low MnO contents and C saturated in FeMn alloy, ending with relatively stable θ_{mg} in both gases for high silicate slag. However, the slag wets the graphite gradually less.

IV. CONCLUSIONS

The wetting behaviour of two immiscible liquids has been studied with the contact and dispensed sessile drop methods. Both methods are valuable to investigate the wetting of the two immiscible liquids. Non-wetting substrate, *i.e.* graphite has less influence on two-liquid wetting study. However, to form a metal bath in a cup, a material which is wetted by the liquid should be chosen.

Parameters which influence the wetting properties are investigated. At temperature up to 100 K above their melting points, the wetting of FeMn alloy and slag does not alter according to temperature, droplet size, and atmosphere, where the slag and metal compositions are still close to initial compositions with almost no reaction happened yet. With increasing of temperature, most likely, reduction of MnO in slag by dissolved C in metal dominates with continuous C supply from the graphite in Ar. Pure CO accelerates the reduction by sweeping away CO_2, even though this is limited in FeMn process. Thus, slag-metal wettability changes with the chemical

OPEN ACCESS

third party material in this article are included in the article's Creative Commons licence, unless indicated otherwise in a credit line to the material. If material is not included in the article's Creative Commons licence and your intended use is not permitted by statutory regulation or exceeds the permitted use, you will need to obtain permission directly from the copyright holder. To view a copy of this licence, visit http://creativecommons.org/licenses/by/4.0/.

REFERENCES

1. S. Olsen, M. Tangstad, and T. Lindstad: *Production of Manganese Ferroalloys*, Tapir Academic Press, Trondheim, 2007, p. 247s.
2. J.H. Park, K.Y. Ko, and T.S. Kim: *Metall. Mater. Trans. B*, 2015, vol. 46B, pp. 741–48.
3. H.S. Jang, J.W. Ryu, and I. Sohn: *Metall. Mater. Trans. B*, 2015, vol. 46B, pp. 606–14.
4. P.A. Eidem, I. Solheim, E. Ringdalen, K. Tang, and B. Ravary, *Proc. of 14th Inter. Ferro. Cong.*, 2015, pp. 190–201.
5. D. Ortiz-Toung, H.C. Chiu, S. Kim, K. Voïtchovsky, and E. Riedo: *Nat. Commun.*, 2013, vol. 4, pp. 1–6.
6. H.S. Kim, J.G. Kim, and Y. Sasaki: *ISIJ Int.*, 2010, vol. 50, pp. 1099–1106.
7. K. Mukai: *ISIJ Int.*, 1992, vol. 32, pp. 19–25.
8. H.B. Zuo, C. Wang, C.F. Xu, J.L. Zhang, and T. Zhang: *Ironmak. Steelmak.*, 2016, vol. 43, pp. 56–63.
9. I.H. Jeong, H.S. Kim, and Y. Sasaki: *ISIJ Int.*, 2013, vol. 53, pp. 2090–98.
10. K. Nakashima and K. Mori: *ISIJ Int.*, 1992, vol. 32, pp. 11–18.
11. T.W. Kang, S. Gupta, N. Saha-Chaudhury, and V. Sahajwalla: *ISIJ Int.*, 2005, vol. 45, pp. 1526–35.
12. S. Bao, *Filtration of Aluminium-Experiments, Wetting, and Modelling*. Ph. D Thesis, The Norwegian University of Science and Technology, 2011.
13. C.H.P. Lupis: *Chemical Thermodynamics of Materials*, Prentice-Hall Inc, New York, 1983.
14. J.V. Naidich, Academic Press, New York, 1981, vol. 420.
15. S. Bao, K. Tang, A. Kvithyld, M. Tangstad, and T.A. Engh: *Metall. Mater. Trans. B*, 2011, vol. 42B, pp. 1358–66.
16. D. Seveno, T.D. Blake, S. Goossens, and J.D. Coninck: *Langmuir*, 2011, vol. 27, pp. 14958–67.
17. S. Bublik, S. Bao, M. Tangstad, and K.E. Einarsrud, *Liq. Met. Proc. Cas. Conf.*, Birmingham, UK, 2019, pp. 375–84.
18. A. Kudyba, N. Sobczak, J. Budzioch, W. Polkowski, and D. Giuranno: *Mater. Des.*, 2018, vol. 160, pp. 915–17.
19. N. Sobczak, R. Nowak, W. Radziwill, J. Budzioch, and A. Glenz: *Mater. Sci. Eng. A*, 2008, vol. 495, pp. 43–49.
20. C.A. Schneider, W.S. Rasband, and K.W. Eliceiri: *Nat. Methods*, 2012, vol. 9, pp. 671–75.
21. C.W. Bale, P. Chartrand, S.A. Degterov, G. Eriksson, K. Hack, R.B. Mahfoud, J. Melançon, A.D. Pelton, and S. Petersen: *Calphad*, 2002, vol. 26, pp. 189–228.
22. S. Bublik, S. Bao, M. Tangstad, and K.E. Einarsrud, *Metall. Mater. Trans. B*, 2021, p. Submitted.
23. T. Tanaka, H. Goto, M. Nakamoto, M. Suzuki, M. Hanao, M. Zeze, H. Yamamura, and T. Yoshikawa: *ISIJ Int.*, 2016, vol. 56, pp. 944–52.
24. S. Bublik and K.E. Einarsrud, *14th Inter. Conf. on CFD in the Oil & Gas*, 2020.
25. H. Kaffash: *Dissolution Kinetics of Carbon Materials in FeMn*, Norwegian University of Science and Technology, Trondheim, 2019.
26. J. Safarian, G. Tranell, L. Kolbeinsen, M. Tangstad, S. Gaal, and J. Kaczorowski: *Metall. Mater. Trans. B*, 2008, vol. 39B, pp. 702–12.
27. I.A. Aksay, C.E. Hoge, and J.A. Pask: *J. Phys. Chem.*, 1974, vol. 78, pp. 1178–83.